Biosensors and Bioelectronics 54 (2014) 679–686

Contents lists available at ScienceDirect

Biosensors and Bioelectronics

journal homepage: www.elsevier.com/locate/bios

An oligofluorene truxene based distributed feedback laser for biosensing applications ☆

Anne-Marie Haughey [a,*], Benoit Guilhabert [a], Alexander L Kanibolotsky [b], Peter J Skabara [b], Martin D Dawson [a], Glenn A Burley [b,*], Nicolas Laurand [a,*]

[a] Institute of Photonics, SUPA, University of Strathclyde, Glasgow G4 0NW, UK
[b] WestCHEM, Department of Pure and Applied Chemistry, University of Strathclyde, Glasgow G1 1XL, UK

ARTICLE INFO

Article history:
Received 4 October 2013
Received in revised form
14 November 2013
Accepted 18 November 2013
Available online 25 November 2013

Keywords:
Organic
Laser
Biosensor
Oligofluorene truxene

ABSTRACT

The first example of an all-organic oligofluorene truxene based distributed feedback laser for the detection of a specific protein–small molecule interaction is reported. The protein avidin was detected down to 1 μg mL^{-1} using our biotin-labelled biosensor platform. This interaction was both selective and reversible when biotin was replaced with desthiobiotin. Avidin detection was not perturbed by Bovine Serum Albumin up to 50,000 μg mL^{-1}. Our biosensor offers a new detection platform that is both highly sensitive, modular and potentially re-usable.

1. Introduction

Evanescent optical sensors are analytical devices that measure changes in refractive index at the device surface. These sensors are highly attractive medical diagnostic platforms for the following reasons: (i) they provide a sensitive platform for the label-free detection of a range of analytes, possibly in real-time, (ii) they offer the potential for the detection of multiple analytes (multiplexing), (iii) they can be integrated into lab-on-chip devices and (iv) their photon-based detection method is non-contact and non-destructive. The latter characteristic gives optical biosensors a number of distinct advantages over sensors based on other transducer technologies, such as electrochemical or acoustic sensors, including unrivaled sensitivity and imperviousness to extraneous effects such as disturbance from ionizing radiation and stray impedances (Ramsden, 1997). Optically pumped distributed feedback (DFB) laser sensors represent an important category of evanescent optical biosensor and have significant potential as a versatile platform technology for the detection of biomolecules. Like other surface sensors, DFB laser sensors can be primed to detect specific analytes by functionalizing the device surface with probe molecules that selectively bind to the analyte of interest (Lu et al., 2008b; Tan et al., 2012). A change in the laser emission wavelength, as a function of analyte binding to the probe, is then used as the signal transduction event. As these sensors are based on an active cavity, where light generated close to resonance with the DFB cavity is amplified by stimulated emission, the resulting laser emission is spectrally narrow. Therefore, high spectral resolution can be achieved in parallel with excellent sensitivity (Tan et al., 2012). Furthermore, because the sensor generates and outputs its own coherent light for sensing, precise and cumbersome optical alignment (required for many optical sensors, microresonator-based evanescent sensors and plasmonic sensors for example Armani et al., 2007; Vollmer et al., 2002) is not necessary, potentially reducing the footprint and cost of the device (Tan et al., 2012; Yang et al., 2008).

We present in this work, for the first time to our knowledge, an all-organic DFB laser biosensing platform using an *organic semiconductor gain medium*. This provides highly sensitive analyte detection which, importantly, is shown to be *reversible*. The specific organic semiconductor used is composed of neat fluorescent tris(terfluorenyl)truxene (T3) which is a monodisperse star-shaped oligomer (Kanibolotsky et al., 2004). In comparison to conjugated polymers, monodisperse oligomers are characterized by well-defined and uniform molecular structure as well as superior chemical purity, characteristics that are critical to the

* Corresponding authors. Tel.: +44 141 548 4120.
E-mail addresses: annemarie.haughey@strath.ac.uk (A.-M. Haughey), benoit.guilhabert@strath.ac.uk (B. Guilhabert), alexander.kanibolotsky@strath.ac.uk (A. L Kanibolotsky), peter.skabara@strath.ac.uk (P. J Skabara), m.dawson@strath.ac.uk (M. D Dawson), glenn.burley@strath.ac.uk (G. A Burley), nicolas.laurand@strath.ac.uk (N. Laurand).

0956-5663/$ - see front matter © 2013 The Authors. Published by Elsevier B.V. All rights reserved.
http://dx.doi.org/10.1016/j.bios.2013.11.054

performance and reproducibility of our DFB laser sensors. Furthermore, the advantages of using an organic semiconductor as the gain material, rather than the dye-doped polymers of current DFB laser sensors (Lu et al., 2008a, 2008b), include high resistance to photo-emission quenching, excellent thin film processability and a higher refractive index (Díaz-García et al., 1997). The latter results in a higher confinement of the laser mode and to an enhancement of the evanescent field interaction with the laser surface and hence sensitivity. Recently we reported that bulk solution refractive index changes can be detected with a T3 DFB laser sensor and that the sensor surface is amenable to adsorption of polyelectrolytes (Haughey et al., 2013). We have also demonstrated that the layer-by-layer adsorption of polyelectrolytes continued to be resolved beyond a stack thickness of 40 nm. The 'plastic' nature of our DFB laser devices means that large scale production is straight-forward, as they can be fabricated using well established solution-processing and soft material patterning processes (Guilhabert et al., 2010; Ge et al., 2010). In addition, plastic DFB laser sensors can also be integrated into existing assay equipment, such as microtiter plates, which are routinely used for high-throughput biosensing measurements (Tan et al., 2012).

Herein we demonstrate that the addition of a polyphenylalanine lysine (PPL) polymer monolayer, onto the T3 gain layer, provides solvent-accessible functional groups for functionalization with a biotin probe that can detect avidin down to 1 μg mL^{-1}. The avidin/biotin system was used to demonstrate biomolecular analyte/receptor interaction at the sensor surface as it has a low dissociation constant (K_d) of $\approx 10^{-15}$ M and therefore produces a very stable biotin–avidin complex (Green, 1975). Furthermore, we show that detection of avidin is both specific and reversible by functionalizing the surface with desthiobiotin, which has a lower affinity for avidin, and observe avidin release from the desthiobiotin surface by the addition of biotin, demonstrating the potential to 're-use' this sensor.

2. Methods

2.1. Materials

PPL (MW 20,000–50,000), poly-L-lysine (PL) (MW 30,000–70,000), polyethyleneimine (PEI) (MW 750,000), phosphate buffered saline (PBS) tablets, sodium chloride (NaCl) tablets, bovine serum albumin (BSA) and Dimethyl Sulfoxide (DMSO) were purchased from Sigma Aldrich. Toluene, avidin and sulfo-N-hydroxysuccinimide biotin (NHS-biotin) were purchased from Fisher Scientific UK. N-hydroxysuccinimide desthiobiotin (NHS-desthiobiotin) was purchased from Berry&Associates Inc. T3 is synthesized in-house. The structures of the T3, polyelectrolytes, NHS-biotin and NHS-desthiobiotin used in this study are shown in Fig. 1. Norland 65 (optical epoxy used for laser substrate) was acquired from Norland Products. Water for experiments was purified by a Milli-Q system (Millipore). All chemicals were used as received. Silica master gratings were fabricated to our design at MC2, Chalmers University, Sweden. A custom-made demountable cuvette used throughout the study, was purchased from Comar Instruments.

2.2. Fabrication of DFB laser device

The diffraction grating imprinted substrate was obtained by replicating a silica master grating into a photo-curable optical epoxy. For this, the Norland 65 was drop-coated onto a silica master grating surface and a 15 mm x 15 mm commercially available acetate sheet of 0.1 mm thickness was placed on top of the epoxy. The epoxy was photo-cured with a UV lamp for 50 s, (exposure dose ≈ 300 J cm^{-2}, spectrum centred at 370 nm) and the grating-imprinted epoxy was peeled from the master grating. The epoxy/acetate sheet was trimmed to ≈ 7 mm $\times$ 12 mm and further curing of the substrate was performed under the UV lamp for an additional 60 min. Just prior to use, the grating-imprinted epoxy was fixed to the flat surface of a demountable cuvette using a drop of Norland 65 and cured for 4 minutes with the UV lamp.

A toluene solution of T3 (20 mg mL^{-1}) was spin-coated on the surface of the grating imprinted epoxy at 3.2 krpm for 90 s. Toluene is reported to have no effect on the cured epoxy, therefore, we do not expect any deformation of the grating structure (Norland, 2013). The thickness of the T3 layer for a range of spinning speeds has been investigated to optimize laser operation for single transverse mode emission and the maximum shift in Bragg wavelength for each unit change in superstrate refractive index. A speed of 3.2 krpm resulted in a T3 layer thickness of $\approx 70 \pm 10.0$ nm and $> 95\%$ of devices fabricated demonstrate single transverse mode (TE_0) emission.

2.3. Fabrication of the T3 biosensing platform

In order to exploit the DFB laser for sensing specific analytes, the T3 surface was coated with a polyelectrolyte monolayer (e.g. PPL) to assimilate amine functionality to the sensor surface; biotin groups were then incorporated on the sensor by coupling with NHS-biotin. This method has been used to facilitate detection of a range of analytes (Ruiz-Taylor et al., 2001; Jenison et al., 2001).

2.4. Characterisation of the optical properties of the DFB lasers

The beam of a frequency-tripled, Q-switched Nd:YAG laser (355 nm, 10 Hz repetition rate, 5 ns pulses) was used to excite the laser sensor, fixed within the demountable cuvette, with a spot of ≈ 24 μm by ≈ 50 μm. Measurements of emission from the laser sensor were performed by photopumping the sensor structure through the glass cuvette and epoxy substrate, at an angle of $\approx 45^\circ$ to the surface normal. Pumping at an angle of $\approx 45^\circ$ to the surface normal is done to make collection of laser emission (which is normal to the sensor surface) as simple as possible. The lasers could be pumped transversally, i.e. in the direction perpendicular to the organic thin-film. In other words, 'coupling' *per se* of the pump into the film plane is not necessary. The only requirement is that the pump hits an area of the laser (within the 5 $\times$ 5 mm active surface). Vertical outcoupled emission through the substrate was collected via a 50−μm core optical fiber, positioned normal to the cuvette surface. The fiber was connected to a grating-coupled CCD spectrometer channel that had a resolution of 0.13 nm.

2.5. Specific avidin detection

Polyelectrolyte functionalized surfaces were achieved using similar protocols reported previously (Al-Hakim and Hull, 1986; Kim et al., 2005). PEI was prepared in 0.9 M NaCl to a concentration of 5 mg mL^{-1}. The laser sensor was washed with 0.9 M NaCl before immersing the laser in PEI solution for 10 min. After removal of the PEI solution, the sensor was washed with NaCl and then 10 mM pH 7.4 PBS. The emission wavelength from the sensor, whilst immersed in PBS, was recorded. NHS-biotin, dissolved in 10 mM PBS to a concentration of 0.2 mg mL^{-1}, was added to the cuvette for 20 min. The emission wavelength was recorded upon adding and prior to removal of the biotin solution. The NHS-biotin solution was removed and the cuvette was washed with PBS before recording the emission wavelength in PBS. A dilution series of Avidin (1–500,000 ng mL^{-1}) in 10 mM PBS was used to determine the limit of detection of the sensing platform. The emission wavelength was recorded upon immersion

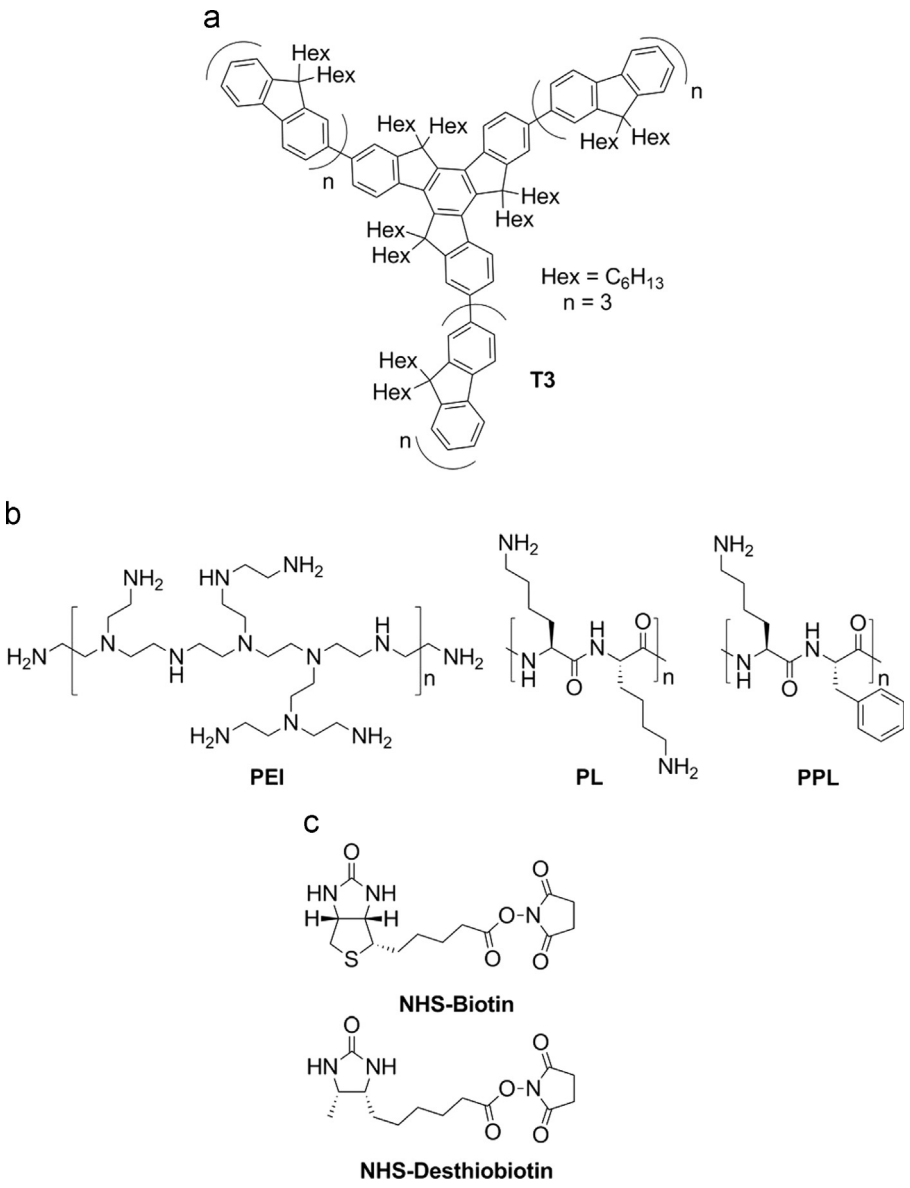

Fig. 1. Chemical structures of the compounds used in this study: oligofluorene truxene (a), polyelectrolytes (b) and biotins (c).

of the sensor in avidin solution and after 20 min, just prior to removal of the solution. The sensor was washed with PBS and the final emission wavelength recorded in PBS. This process was repeated, with a different laser sensor, for each of the avidin concentrations.

This general protocol was used for the fabrication of the T3 layer with PPL and PL in place of PEI. PPL and PL solutions were at a concentration of 1 mg mL^{-1} in 10 mM PBS therefore, PBS was used in place of NaCl. The shift in wavelength produced by each avidin concentration was determined by subtracting the emission wavelength recorded in PBS, prior to the addition of avidin solution, from the final emission wavelength recorded in PBS. The relative shift in wavelength demonstrates the shift due to the presence of avidin remaining bound to the biotin functionalized laser surface after washing.

In order to determine the avidin limit of detection for each of the polyelectrolyte-biotin functionalized sensors, repeated measurements ($4\times$) of avidin binding (10 μg mL^{-1}) were performed on different lasers. The standard deviation of the shift in wavelength attributed to avidin binding of these independent measurements was 0.02 nm. A shift in wavelength is deemed to be 'detectable' if it has a magnitude of three times the standard deviation (Cunningham, 2008). Therefore, the minimum level of avidin detection is defined as the avidin concentration resulting in a shift in wavelength $\geq$ 0.06 nm.

2.6. Reversible specific avidin detection

Sensors were functionalized with PPL and desthiobiotin as described in Section 2.4 for a PPL functionalized sensor. A solution of NHS-desthiobiotin in DMSO was added to 10 mM PBS to a concentration of 0.2 mg mL^{-1}, with a final DMSO concentration of 2% v/v.

10 mM PBS solution was used for all wash steps prior to and following immersion of the sensor in avidin/biotin. The relative shift in emission wavelength for the demonstration of reversible avidin sensing and for determining the avidin limit of detection was obtained as described in Section 2.4.

2.7. Investigation of non-specific protein adsorption using BSA

The non-specific adsorption of BSA to our PPL, PPL-biotin and PPL-desthiobiotin functionalized sensor was investigated for four BSA concentrations (1, 10, 500 and 50,000 μg mL^{-1}). BSA solutions were prepared in 10 mM PBS. Sensors were coated with PPL as previously described in Section 2.4. The emission wavelength, with the sensor immersed in PBS, was recorded. A BSA solution was then added to the cuvette and the emission wavelength recorded. After 20 min, the emission wavelength was recorded again before removing the BSA solution from the cuvette. The sensor was washed with PBS before a final emission wavelength was recorded with the sensor immersed in PBS. This was repeated for each BSA concentration, with a new sensor for each measurement, and was performed three times for each BSA concentration. The procedure was also repeated for a PPL-biotin and PPL-desthiobiotin functionalized sensor.

Competition assays using BSA and avidin were performed with a PPL-biotin and a PPL-desthiobiotin functionalized laser sensor. A range of BSA concentrations (1–50,000 μg mL^{-1}), with 2.5 μg mL^{-1} avidin, were prepared in 10 mM PBS. The relative shift in wavelength due to BSA and/or avidin was determined in the same way as described for BSA.

3. Results and discussion

3.1. Principles of DFB laser structure and operation

The structure of our DFB laser is shown in Fig. 2a. This sensing platform has a three-layer planar waveguide structure with a thin gain layer sandwiched between substrate (optical epoxy, see Methods) and superstrate (e.g. surface adsorbed molecules and buffer solution) regions. The surface of the substrate is nanopatterned with a grating structure of 276 nm period (Λ) and $\approx$50 nm modulation depth. The organic semiconductor gain layer is composed of T3 (Fig. 1a). The structure of T3 is a monodisperse star-shaped oligomer which has high photoluminescence quantum yields in both solution and the solid-state, and forms low-loss waveguiding films onto a substrate when deposited from solution (Guilhabert et al., 2010; Kanibolotsky et al., 2004; Herrnsdorf et al., 2010; Tsiminis et al., 2009). T3 has peak absorbance at 370 nm with photoluminescence emission peaks at 425 and 442 nm. For sensor operation, the T3 molecules are optically excited by a pulsed UV (355 nm) pump laser. The refractive index of T3 is 1.81 at 430 nm in a thin film, which is higher than the refractive indices of the substrate and superstrate (Tsiminis et al., 2009). This change in refractive index results in the confinement of light within the gain layer by total internal reflection, i.e. forming a planar waveguide, which is 'perturbed' by the nanostructure. The periodicity of the nanostructure provides both the out-coupling and feedback mechanism for the laser modes through first and second diffraction orders, respectively.

Laser emission from the DFB laser sensor is described by the Bragg equation, Eq. (1), where λ is the Bragg wavelength (emission from the laser is at, or close to, this wavelength), n_{eff} is the effective refractive index of the laser mode and is dependent on the refractive indices for each of the three layers of the DFB laser structure and the gain layer thickness, and Λ is the grating period as defined previously:

$$\lambda = n_{eff}\Lambda \tag{1}$$

The periodic nanostructure imprinted in our sensor substrate is a second-order grating, which causes counter-propagating modes to couple through the second order of diffraction while first order modes are coupled vertically out of the laser structure, as shown in Fig. 2a. It is this out-coupled laser emission that can be detected for wavelength monitoring and hence sensing.

Eq. (1) demonstrates that changes in the effective refractive index result in a change in the wavelength of emission from the DFB laser. n_{eff} depends on parameters, which are all fixed except for the refractive index of the superstrate. Therefore, changes in the optical properties at the laser surface correlate with shifts in the emission wavelength of the laser.

3.2. Optical characterization

The laser emission spectrum observed for a sensor immersed in PBS solution, functionalized with PPL and biotin, and after exposure to 2.5 μg mL^{-1} avidin solution, is shown in Fig. 3. Emission from all laser sensors was at the resolution limit of the spectrometer used (0.13 nm). The central wavelength and linewidth were determined from a Gaussian fit to the data. As the linewidth of laser emission was at, or below, the limit of the spectrometer resolution, spectra were fitted using either two or three data points above the noise (Fig. 3). Data fitting provided the best estimate of the central wavelength and linewidth within the current spectrometer limitations (Ge et al., 2010). The spectral linewidth of laser emission remaining narrow after functionalization with PPL and biotin, and exposure to avidin, demonstrated that the further addition of monolayers on the sensor surface did not compromise the characteristics of the laser emission. The inset

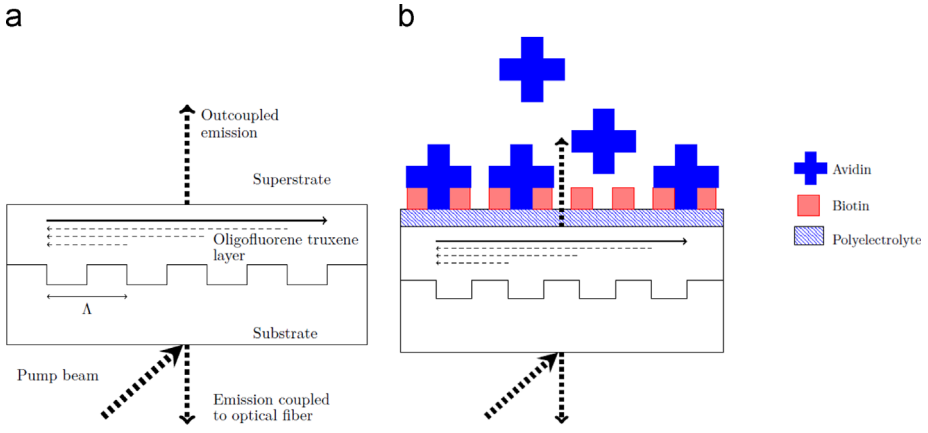

Fig. 2. Schematic illustration of our DFB laser biosensor (a) and functionalization of the sensor surface with polyelectrolyte and biotin for avidin sensing (b). The dashed and arrowed lines within the structure represent feedback from successive periods of the grating.

in Fig. 3 shows the relationship between the laser emission intensity and the pump beam energy, with the sensor exposed to air, demonstrating a threshold energy of 2.5 nJ, corresponding to a fluence of 60 μ J cm^{-2} with 5 ns pulse duration. Our group has previously reported on the lifetime of T3 DFB lasers identical to those described in this paper (Foucher et al., 2013). Lifetime measurements indicated that when submerged in water, the laser remained operational beyond exposure to 10,000 pulses, with a pulse fluence approximately 250 times that of the threshold fluence. 10,000 pulses correspond to a period of time >15 min. As each measurement with our laser sensor corresponds to pumping the sensor for a maximum of 5 s, the laser should allow for >200 measurements at one particular location on the laser. It should be noted that sensing measurements are performed at a fluence closer to that of the laser threshold, therefore, the estimate of 200 measurements is greatly underestimated. It has also been reported that the emission wavelength of the laser remains constant over time (Haughey et al., 2013), even as the intensity of the laser emission diminishes (Foucher et al., 2013).

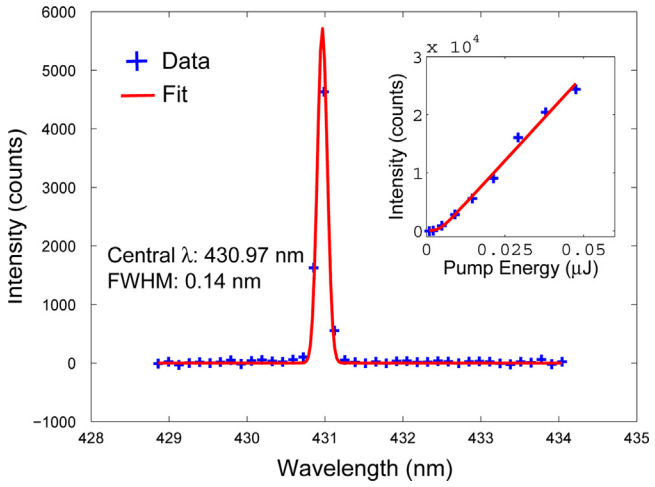

Fig. 3. Spectral emission from a laser functionalized with PPL and biotin, and after exposure to 2.5 μg mL^{-1} avidin. Inset shows the oscillation threshold (2.5 nJ) for a DFB laser in air.

3.3. Specific detection of avidin

Our approach to functionalization of the sensor surface and subsequent specific detection of avidin is the focus of the remainder of Section 3. Functionalization of the sensor surface for avidin detection is illustrated schematically in Fig. 2b. We present results demonstrating the effect the chosen polyelectrolyte layer, used for functionalization of the sensor, has on avidin detection in Section 3.4. Our demonstration of reversible avidin detection is detailed in Sections 3.5 and 3.6 presents our investigation into the non-specific adsorption of proteins to the sensor surface.

Functionalization of our DFB laser sensor with biotin was achieved by adsorption of a polyelectrolyte containing amine groups and subsequent functionalization with NHS-biotin (Erol et al., 2006). Three polyelectrolytes (PEI, PL and PPL), with chemical structures shown in Fig. 1b, were explored in order to survey which polymer would provide the greatest level of biotin functionalization and thus the lowest limit of detection for avidin sensing. The chemical structures for NHS-biotin and the three polyelectrolytes used in this study are shown in Fig. 1c.

Branched PEI was previously used as the base monolayer for stacking of alternately charged polyelectrolytes and was therefore the initial polyelectrolyte chosen to investigate biotin functionalization (Haughey et al., 2013). The primary amine groups of PEI enabled facile functionalization with the activated ester of NHS-biotin. A number of DFB laser sensors were functionalized with PEI and biotin and the average relative shift in emission wavelength (with the non-functionalized laser as reference), attributed to biotin covalently linked to the sensor surface, was 0.17 ± 0.07 nm. Each of these sensors were subsequently exposed to an

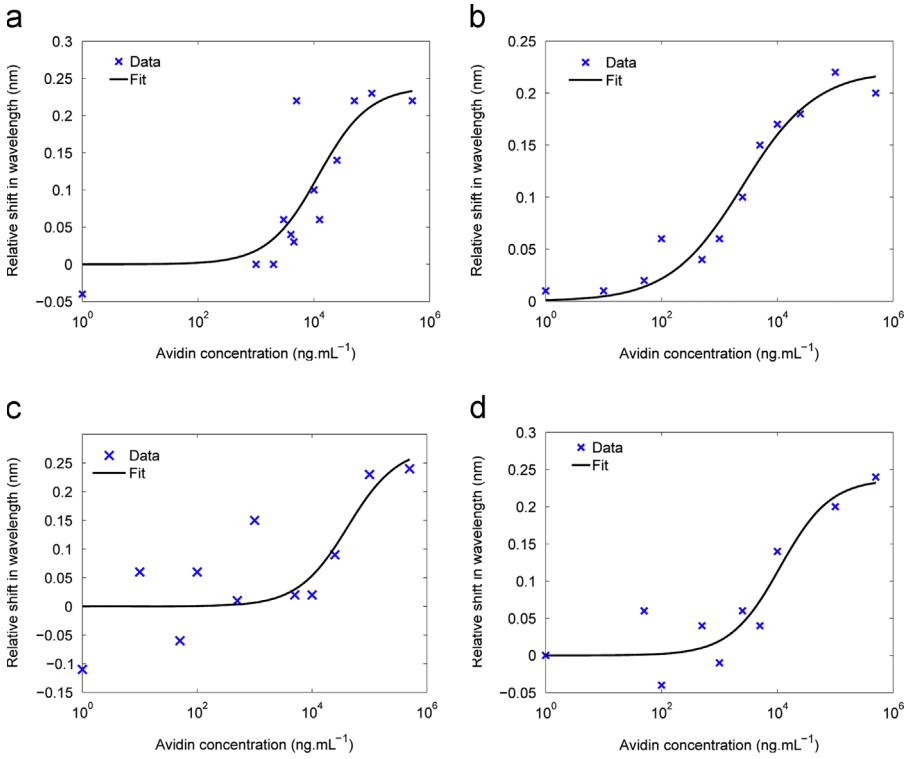

Fig. 4. Specific avidin sensing study for sensors functionalized with biotin and PEI (a), PPL (b), PL (c) and desthiobiotin and PPL (d). The data was fitted using Eq. (2).

avidin solution over a range of concentrations. The relative shifts in emission wavelength after exposure to each avidin concentration are shown in Fig. 4a. The data in Fig. 4a was fitted using the Michaelis–Menten equation (Attie and Raines, 1995):

$$y = \frac{B_{max} \cdot x}{K_d + x} \quad (2)$$

Eq. (2) can be used to describe protein binding reactions, where y is the relative shift in wavelength corresponding to avidin binding to sensor surface, B_{max} represents the maximum relative shift in wavelength, which is directly proportional to the maximum binding capacity of the biotin functionalized sensor, x is the avidin concentration and K_d is the dissociation constant that represents the avidin concentration for which the number of avidin molecules bound to the sensor surface results in a shift of $B_{max}/2$. The avidin limit of detection for a PEI-biotin functionalised DFB laser sensor was $\approx 5\ \mu g\ mL^{-1}$ and a dissociation constant of 2.0^{-7} M, the R-squared value for the fit to the data was 0.83.

In order to test the specificity of avidin detection, an avidin binding assay was performed on a DFB laser sensor functionalized with PEI alone. A 100 $\mu g\ mL^{-1}$ avidin solution, chosen as it results in a maximum shift in wavelength for a biotin coated sensor, produced a negative shift in wavelength (-0.12 nm). This relatively large negative shift is presumably due to the extra immersion of the laser sensor in various solutions which may remove more unbound PEI than the standard single wash. We conclude that avidin does not bind to the surface of a PEI coated laser in the absence of subsequent biotin functionalization, indicating that avidin binding for a PEI-biotin functionalized sensor is specific.

Replacing the initial PEI base layer with PPL resulted in an average relative shift in emission wavelength, due to biotin binding to the PPL coated surface, of 0.28 ± 0.09 nm. Fig. 4b shows the relative shift in wavelength for each avidin concentration for PPL-biotin functionalized sensors. There was an improvement in the fit to the data, relative to the fit of data for a PEI-biotin coated sensor, with an R-squared value of 0.98. The avidin limit of detection for a PPL-biotin functionalized laser sensor was $\approx 1\ \mu g\ mL^{-1}$, which is five times lower than the avidin limit of detection for a laser sensor with PEI as the initial monolayer and the corresponding dissociation constant was 3.6^{-8} M.

The specificity of avidin binding was investigated by immersing a PPL functionalized laser in a 25 $\mu g\ mL^{-1}$ avidin solution. This concentration was at the saturation point of avidin detection for a PPL-biotin functionalized sensor. As for the PEI control, there was a negative (-0.17 nm) shift in emission wavelength upon removal of avidin solution indicative of specific binding to the biotin-functionalized monolayer. We hypothesize that the improvement in the limit of detection of avidin when PPL was used in place of PEI was due to the pi-stacking of the phenyl substituents of the phenylalanine groups on the T3 surface. In order to test this hypothesis, the PPL base layer was replaced with PL. The relative shift in emission wavelength for biotin binding at the surface of a PL functionalized sensor was significantly lower than that for a PEI and PPL functionalized sensor, at 0.07 ± 0.07 nm. In addition, there was a significant increase in the variability of the shift in wavelength produced by biotin binding. We infer that the initial PL layer may not be a confluent, uniform monolayer for each sensor, therefore, reducing the density of available amine binding sites which in turn results in a marked increase in variability from sensor to sensor. The avidin detection data for a PL-biotin functionalized sensor is shown in Fig. 4c where the avidin limit of detection was $\approx 50\ \mu g\ mL^{-1}$, an order of magnitude higher than the avidin limit of detection when the sensor was functionalized with PEI. The associated dissociation constant was 6.9^{-7} M. The data also produced a poor fit to the Michaelis–Menten equation, with an R-squared value of 0.80, and a decrease in the dynamic range for avidin detection.

Table 1
Relative shift in wavelength due to biotin coupling to sensors functionalized with PEI, PPL or PL and desthiobiotin coupling to a PPL functionalized sensor, the corresponding avidin limit of detection for each of those sensors and the dissociation constants extracted from the Michaelis–Menten fit to the data.

Polyelectrolyte	Relative shift in wavelength		Avidin limit of detection ($\mu g\ mL^{-1}$)	Dissociation const. (M)
	Biotin coupling (nm)	Desthiobiotin coupling (nm)		
PEI	0.17 ± 0.07		5	2.0^{-7}
PPL	0.28 ± 0.09		1	3.6^{-8}
PL	0.07 ± 0.07		50	6.9^{-7}
PPL		0.14 ± 0.08	2.5	1.8^{-7}

We therefore conclude that functionalization of the sensor with PPL resulted in the lowest avidin limit of detection; the results are summarized in Table 1. A base layer of PEI resulted in a significant increase in avidin limit of detection, relative to that of PPL, at 1 $\mu g\ mL^{-1}$ and a limit of detection of 50 $\mu g\ mL^{-1}$ when PL was used. The differences in the limit of detection values correlate with the relative shift in emission wavelength attributed to biotin coupling. A redshift in emission wavelength is a result of an increase in the effective refractive index of the sensor, as described in Eq. (1). Therefore, the area density of biotin molecules bound to the sensor surface correlates to the magnitude of the relative shift in wavelength detected, i.e. higher levels of biotin coupling result in a greater redshift in emission wavelength. The greatest relative shift in emission wavelength for biotin coupling, 0.28 ± 0.09 nm, was observed when PPL was used for the base layer and the smallest shift, 0.07 ± 0.07 nm, was observed when PL was used for the initial layer. We therefore infer that the sensor surface is functionalized with the greatest number of biotin molecules when PPL is used as the polyelectrolyte base layer.

There is no direct comparison available in the literature for specific avidin detection achieved with a DFB laser sensor. TNF-α and Human IgG antibody detection has been reported for a dye-doped DFB laser sensor, with detection limits of 0.6 $\mu g\ mL^{-1}$ and $\approx 0.5\ \mu g\ mL^{-1}$, respectively (Tan et al., 2012; Lu et al., 2008a). Avidin detection with a biotin functionalized sensor has previously been reported for a number of photonic biosensors, e.g. microring and slotted photonic crystal based sensors (Scullion et al., 2011; DeVos et al., 2007), where the avidin limit of detection is in the range of 0.01–1 $\mu g\ mL^{-1}$, demonstrating that the detection limit for avidin of our laser is comparable to waveguide based devices. We note that the sensitivity of our laser sensor could be markedly improved by optimizing the spectral measurement in order to increase the detection resolution. Further improvements in sensitivity may also be achieved by optimizing the sensor structure, for example reducing the refractive index of the substrate to match that of the superstrate layer would result in a more symmetric structure and would cause a greater overlap between the laser mode and the sensing region (Haughey et al., 2013).

3.4. Reversible specific avidin detection

Due to the strong binding affinity of biotin–avidin ($K_d \approx 10^{-15}$ M), a combination of extreme conditions, such as high temperature and low pH, are required to release avidin from the surface. For many applications, irreversible binding will be a distinct advantage as the risk of disruption to binding events is minimized. However, reversing binding events is desirable if the assay is to be repeated thus rendering the sensor platform

're-usable'. Desthiobiotin (structure shown in Fig. 1c) is a biotin analogue with a lower binding affinity ($K_d \approx 10^{-11}$ M) for avidin and has been used in reversible avidin binding assays (Hirsch et al., 2002; Wong et al., 2013).

As the lowest avidin limit of detection was achieved for a laser functionalized with an initial layer of PPL, PPL was the polyelectrolyte used to investigate the capacity of reversible binding of a desthiobiotin–avidin binding using our detection platform. Desthiobiotin functionalization of the sensor surface was achieved using NHS-desthiobiotin (Wong et al., 2013). Fig. 5a shows the reversibility of avidin coupling to desthiobiotin. Relative shifts in wavelengths of 0.08, 0.09 and 0.09 nm were observed after each exposure to avidin solution (10 μg mL^{-1}). Upon removal of avidin solution and a PBS wash, the sensor was immersed in a biotin solution (0.2 mg mL^{-1}) where the associated relative shifts in wavelength after exposure to the biotin solutions were −0.05, −0.06 and −0.13 nm. Fig. 5a clearly shows that most of the avidin bound to the desthiobiotin functionalized sensor was removed after immersion in the biotin solution and that avidin binding to the desthiobiotin layer was reproducible. When biotin was used in place of desthiobiotin, the addition of biotin after avidin binding resulted in no change in the emission wavelength from the sensor, indicating that there was no removal of avidin from the sensor and no detectable biotin binding. We surmise that the reversibility of the assay when desthiobiotin was used is due to the lower binding affinity of desthiobiotin (10^{-11} M) to avidin relative to that of biotin (10^{-15} M). Therefore, the immersion of the sensor in a biotin solution leads to the release of avidin upon washing with PBS. This results in a negative shift in the emission wavelength that corresponds to the magnitude of the shift in wavelength attributed to avidin coupling.

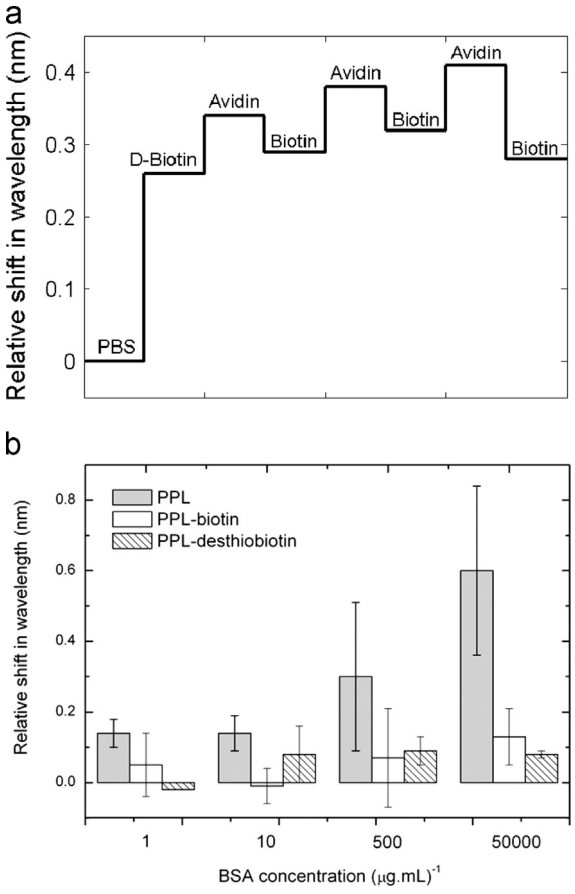

Fig. 5. The shifts in wavelength relative to a baseline PBS wavelength are shown for a sensor functionalized with PPL. The shifts in wavelength attributed to desthiobiotin (D-Biotin) and avidin are shown as well as the relative wavelength upon avidin removal by immersion of the sensor in biotin solution (a). And average relative shift in wavelength attributed to non-specific adsorption of BSA to a sensor functionalized with PPL or PPL and biotin. Error bars represent the standard deviation of the mean (b).

The avidin detection assay was then performed using a PPL-desthiobiotin functionalized sensor. Fig. 4d shows the relative shift in wavelength for each avidin concentration for PPL-desthiobiotin functionalized sensors and the results are included in Table 1. The average relative shift in wavelength due to desthiobiotin binding to the PPL surface was 0.14 ± 0.08 nm. The data in Fig. 4d was fitted to the Michaelis–Menten equation and an *R*-squared value of 0.94. The limit of detection for a PPL-desthiobiotin functionalized sensor was 2.5 μg mL^{-1}, between that of a PEI-biotin and PPL-biotin functionalized sensor and the dissociation constant was 1.8^{-7} M. We therefore conclude that specific, and reversible, avidin detection can be achieved through the replacement of biotin with desthiobiotin for the functionalization of the laser sensor.

3.5. Non-specific BSA adsorption

Non-specific adsorption to our detection platform was then determined using BSA. Albumin is present in abundance in blood samples and could potentially interfere with the detection of specific analytes. Fig. 5b shows the mean response of our sensor, functionalized with either PPL, PPL-biotin or PPL-desthiobiotin, after exposure to BSA solutions of varying concentrations (measured in triplicate). BSA has a pI of 4.7 and is thus negatively charged at pH 7.4. As a result, a significant redshift in emission wavelength was attributed to non-specific adsorption of BSA to the positively charged surface of a PPL coated sensor. There was a reduction in the shift in wavelength across all BSA concentrations for PPL-biotin and PPL-desthiobiotin functionalized laser sensors, presumably as consequence of the biotin layer masking the positive charge of the underlying PPL layer. We assume that this suppresses the electrostatic attraction between the positively charged PPL and negative BSA, which in turn suppresses the non-specific adsorption of BSA to the sensor surface (Williams et al., 2013).

The effect of non-specific adsorption of BSA on specific avidin sensing, with PPL-biotin and PPL-desthiobiotin functionalized sensors, was investigated by performing a competition assay with BSA solutions at a range of concentrations (1–50,000 μg mL^{-1}) containing 2.5 μg mL^{-1} of avidin. No increase in emission wavelength as a function of increasing BSA concentration was observed. The average shift in emission wavelength was 0.09 ± 0.04 nm (biotin) and 0.03 ± 0.05 nm (desthiobiotin). These values correspond to the relative shifts in emission wavelengths observed for detection of 2.5 μg mL^{-1} avidin when no BSA is present (Fig. 4b and d). We therefore conclude that the presence of BSA does not affect the specific detection of avidin even at concentrations comparable to those found in serological samples, and that there was no detectable non-specific adsorption of BSA in the presence of avidin at a concentration of 2.5 μg mL^{-1}. This is an important observation in downstream optimization of the specificity of the DFB laser sensor for specific biosensing applications.

4. Conclusions

We report what is to our knowledge the first application of an oligofluorene truxene based DFB laser sensor for the sensitive detection of biomolecules. Our laser design can be fabricated using well established and scalable processes and does not require precise optical alignment. Furthermore our design can be readily

incorporated into existing assay equipment. The design is highly compatible for biomolecule sensing, with the sensing of avidin used as proof of concept in this study. This detection limit was comparable to existing DFB laser sensors, however further optimization of the sensor, and improvement to the spectrometer resolution, could improve the sensitivity of our sensor even further. The potential for a re-usable sensing system was demonstrated and our chosen system for functionalization of the sensor surface was shown to prevent the non-specific adsorption of BSA up to 50,000 μg mL^{-1}. Future work will focus on optimizing the functionalization of the sensor for the specific detection of nucleic acids, peptides and proteins and miniaturization of the sensing platform to achieve a compact system.

Acknowledgments

The authors gratefully acknowledge financial support by the EPSRC (EP/J021962/1 and EP/I029141/1).

References

Al-Hakim, A.H., Hull, R., 1986. Nucl. Acids Res. 14 (24), 9965–9976.
Armani, A.M., Kulkarni, R.P., Fraser, S.E., Flagan, R.C., Vahala, K.J., 2007. Science 317 (5839), 783–787.
Attie, A.D., Raines, R.T., 1995. J. Chem. Educ. 72 (2), 119.
Cunningham, B., 2008. Label Free Biosensors - Techniques and Applications. Cambridge University Press. pp. 1–28.
Dííaz-García, M.A., Hide, F., Schwartz, B.J., Andersson, M.R., Pei, Q., Heeger, A.J., 1997. Synth. Met. 84 (1–3), 455–462.
DeVos, K., Bartolozzi, I., Schacht, E., Bienstman, P., Baets, R., 2007. Opt. Express 15 (12), 7610–7615.
Erol, M., Du, H., Sukhishvili, S., 2006. Langmuir 22 (26), 11329–11336.
Foucher, C., Guilhabert, B., Kanibolotsky, A., Skabara, P., Laurand, N., Dawson, M., 2013. Optical Mater. Express 3 (5), 584–597.
Ge, C., Lu, M., Jian, X., Tan, Y., Cunningham, B.T., 2010. Opt. Express 18 (12), 12980–12991.
Green, N.M., 1975. Advances in Protein Chemistry, vol. 29. Academic Press, pp. 85–133.
Guilhabert, B., Laurand, N., Herrnsdorf, J., Chen, Y., Mackintosh, A.R., Kanibolotsky, A.L., Gu, E., Skabara, P.J., Pethrick, R.A., Dawson, M.D., 2010. J. Opt. 12 (3), 035503.
Haughey, A.-M., Guilhabert, B., Kanibolotsky, A., Skabara, P., Burley, G., Dawson, M., Laurand, N., 2013. Sens. Actuators B 185 (0), 132–139.
Herrnsdorf, J., Guilhabert, B., Chen, Y., Kanibolotsky, A., Mackintosh, A., Pethrick, R., Skabara, P., Gu, E., Laurand, N., Dawson, M., 2010. Opt. Express 18 (25), 25535–25545.
Hirsch, J.D., Eslamizar, L., Filanoski, B.J., Malekzadeh, N., Haugland, R.P., Beechem, J.M., Haugland, R.P., 2002. Anal. Biochem. 308 (2), 343–357.
Jenison, R., La, H., Haeberli, A., Ostroff, R., Polisky, B., 2001. Clin. Chem. 47 (10), 1894–1900.
Kanibolotsky, A.L., Berridge, R., Skabara, P.J., Perepichka, I.F., Bradley, D.D.C., Koeberg, M., 2004. J. Am. Chem. Soc. 126 (42), 13695–13702, PMID: 15493927.
Kim, M.S., Seo, K.S., Khang, G., Lee, H.B., 2005. Langmuir 21 (9), 4066–4070.
Lu, M., Choi, S.S., Irfan, U., Cunningham, B.T., 2008a. Appl. Phys. Lett. 93 (11), 111113–111113-3.
Lu, M., Choi, S.S., Wagner, C.J., Eden, J.G., Cunningham, B.T., 2008b. Appl. Phys. Lett. 92 (26), 261502.
Norland, 2013. ⟨https://www.norlandprod.com/techrpts/chemresit.html⟩.
Ramsden, J.J., 1997. J. Mol. Recognit. 10 (3), 109–120.
Ruiz-Taylor, L.A., Martin, T.L., Zaugg, F.G., Witte, K., Indermuhle, P., Nock, S., Wagner, P., 2001. Proc. Natl. Acad. Sci. 98 (3), 852–857.
Scullion, M., Falco, A.D., Krauss, T., 2011. Biosens. Bioelectr. 27 (1), 101–105.
Tan, Y., Ge, C., Chu, A., Lu, M., Goldshlag, W., Huang, C.S., Pokhriyal, A., George, S., Cunningham, B., 2012. IEEE Sens. J. 12 (5), 1174–1180.
Tsiminis, G., Wang, Y., Shaw, P.E., Kanibolotsky, A.L., Perepichka, I.F., Dawson, M.D., Skabara, P.J., Turnbull, G.A., Samuel, I.D.W., 2009. Appl. Phys. Lett. 94 (24), 243304–243304-3.
Vollmer, F., Braun, D., Libchaber, A., Khoshsima, M., Teraoka, I., Arnold, S., 2002. Appl. Phys. Lett. 80 (21), 4057–4059.
Williams, E.H., Schreifels, J.A., Rao, M.V., Davydov, A.V., Oleshko, V.P., Lin, N.J., Steffens, K.L., Krylyuk, S., Bertness, K.A., Manocchi, A.K., Koshka, Y., 2013. J. Mater. Res. 28, 68–77.
Wong, N.Y., Xing, H., Tan, L.H., Lu, Y., 2013. J. Am. Chem. Soc. 135 (8), 2931–2934.
Yang, Y., Turnbull, G.A., Samuel, I.D.W., 2008. Appl. Phys. Lett. 92 (16), 163306.